Firat University Journal of Experimental and Computational Engineering

Yeşilyurt Fayı Boyunca Göreli Tektonik Aktivitenin Morfometrik Analizlerle Değerlendirilmesi

Selin SALMAN[1], Yusuf BULUCU[2*], İlknur Fırat AYDIN[3], Abdulrahman ELHİSSO[4], Yaren GÖKTAŞ[5], Fikri AĞGÜN[6], Mehmet KÖKÜM[7]

[1]Acil Durum ve Afet Yönetimi Bölümü, Lisansüstü Eğitim Enstitüsü, Bitlis Eren Üniversitesi, Bitlis, Türkiye.
[2,3]Coğrafya Bölümü, İnsan ve Toplum Bilimleri Fakültesi, Fırat Üniversitesi, Elazığ, Türkiye.
[4]Jeoloji Mühendisliği Bölümü, Mühendislik Fakültesi, Fırat Üniversitesi, Elazığ, Türkiye.
[5]Coğrafya Bölümü, Fen Edebiyat Fakültesi, İnönü Üniversitesi, Malatya, Türkiye.
[6]Bilgisayar Teknolojileri Bölümü, Adilcevaz Meslek Yüksekokulu, Bitlis Eren Üniversitesi, Bitlis, Türkiye.
[4]Jeoloji Mühendisliği Bölümü, Mühendislik Fakültesi, Fırat Üniversitesi, Elazığ, Türkiye.
[1]selin.ilbak@gmail.com, [2]yusufbulucu66@gmail.com, [3]firat.ilknur0244@gmail.com, [4]a.elhisso17@gmail.com, [5]goktasyarenn@gmail.com, [6]faggun@beu.edu.tr, [7]mkokum@firat.edu.tr

Geliş Tarihi: 08.12.2025
Düzeltme Tarihi:17.01.2026
Kabul Tarihi:13.03.2026
doi: https://doi.org/10.62520/fujece.1838507
Araştırma Makalesi

Alıntı: S. Salman, Y. Bulucu, İ. F. Aydın, A. Elhisso, Y. Göktaş, F. Ağgün ve M. Köküm, "Yeşilyurt fayı boyunca göreli tektonik aktivitenin morfometrik analizlerle değerlendirilmesi", Fırat Üni. Deny. Müh. Derg., vol. 5, no 2, pp. 398-417, Haziran 2026.

Öz

Yeşilyurt Fayı (YF), Doğu Türkiye'de yer alan, yaklaşık 70 km uzunluğunda, KD–GB doğrultulu ve sol yanal doğrultu atımlı bir fay olup, Malatya ili için bölgesel sismik tehlikenin değerlendirilmesinde önemli bir yapısal unsuru temsil etmektedir. Bu çalışma, YF boyunca ve ilişkili drenaj havzalarında tektonik aktivitenin mekânsal değişkenliğini nicel olarak değerlendirmek amacıyla çok sayıda morfometrik indisi bir araya getirmektedir. Morfometrik analizler; dağ önü sinüozitesi (Smf), vadi tabanı genişliği–vadi yüksekliği oranı (Vf), hipsometrik eğri (HC) ve hipsometrik integral (HI), asimetri faktörü (AF) ve akarsu uzunluk–eğim indeksi (SL) kullanılarak gerçekleştirilmiştir. Bu indeksler, göreli tektonik aktiviteyi, yükselimi, havza eğimini ve topografik evrimi değerlendirmek amacıyla dört fay segmenti (S1–S4) boyunca dağılan drenaj havzalarına uygulanmıştır. Ayrıca, ampirik fay uzunluğu–moment büyüklüğü ilişkileri kullanılarak tekil segmentlerin ve tüm fay zonunun sismik potansiyeli tahmin edilmiştir. Elde edilen sonuçlar, S1, S2 ve S3 segmentlerinin orta ile görece yüksek düzeyde tektonik aktivite ile karakterize edildiğini; bunun orta düzey Smf ve Vf değerleri, yüksek SL indeksleri ve 0.05–0.5 mm/yıl arasında değişen yükselim hızları ile yansıtıldığını göstermektedir. Buna karşılık, S4 segmenti, 0.05 mm/yıl'ın altındaki yükselim hızları ile görece daha düşük tektonik aktivite sergilemekte olup, bu durumun artmış aşınım süreçleri ve yaygın alüvyal yelpaze gelişimi tarafından kontrol edildiği düşünülmektedir. Hipsometrik analizler, havza evriminde genç, olgun ve yaşlı jeomorfolojik evreler arasında belirgin mekânsal değişkenlik ortaya koyarken, AF sonuçları drenaj havzalarının yaklaşık %80'inin asimetrik geometri sergilediğini ve aktif tektonik eğimi işaret ettiğini göstermektedir. Hesaplanan göreli tektonik aktivite (Iat) indeksleri de S1, S2 ve S3 segmentlerinin yüksek tektonik aktiviteye sahip olduğunu, S4 segmentinin ise orta düzeyde aktivite gösterdiğini doğrulamaktadır. 6 Ekim 2024 tarihinde meydana gelen Mw 6,0 büyüklüğündeki deprem, YF'nin güncel tektonik aktivitesini doğrulamaktadır. Morfometrik sonuçlar ve tüm fayın kırılması durumunda yaklaşık Mw ~7,2 büyüklüğünde bir deprem potansiyeline işaret eden ampirik tahminler birlikte değerlendirildiğinde, YF bölge için önemli bir sismik tehlike oluşturmaktadır.

Anahtar kelimeler: Deprem, Malatya, Morfometrik analiz, Sismik tehlike, Tektonik

*Yazışılan Yazar

İntihal Kontrol: Evet – Turnitin
Şikayet: fujece@firat.edu.tr

Firat University Journal of Experimental and Computational Engineering

Evaluation of the Relative Tectonic Activity of the Yeşilyurt Fault Using Morphometric Analyses

Selin SALMAN[1], Yusuf BULUCU[2*], İlknur Fırat AYDIN[3], Abdulrahman ELHİSSO[4], Yaren GÖKTAŞ[5], Fikri AĞGÜN[6], Mehmet KÖKÜM[7]

[1]Department of Emergency and Disaster Management, Graduate School of Education, Bitlis Eren University, Bitlis, Türkiye.
[2, 3]Department of Geography, Faculty of Humanities and Social Sciences, Fırat University, Elazığ, Türkiye.
[4]Department of Geological Engineering, Faculty of Engineering, Fırat University, Elazığ, Türkiye.
[5]Department of Geography, Faculty of Arts and Sciences, İnönü University, Malatya, Türkiye.
[6]Department of Computer Technologies, Adilcevaz Vocational School, Bitlis Eren University, Bitlis, Türkiye.
[4]Department of Geological Engineering, Faculty of Engineering, Fırat University, Elazığ, Türkiye
[1]selin.ilbak@gmail.com, [2]yusufbulucu66@gmail.com, [3]firat.ilknur0244@gmail.com, [4]a.elhisso17@gmail.com, [5]goktasyarenn@gmail.com, [6]faggun@beu.edu.tr, [7]mkokum@firat.edu.tr

Geliş Tarihi:08.12.2025 Düzeltme Tarihi:17.01.2026 doi: https://doi.org/10.62520/fujece.1838507
Kabul Tarihi: 13.03.2026 Araştırma Makalesi

Citation: S. Salman, Y. Bulucu, İ. F. Aydın, A. Elhisso, Y. Göktaş, F. Ağgün and M. Köküm "Evaluation of the relative tectonic activity of the yeşilyurt fault using morphometric analyses", Firat Univ. Jour.of Exper. and Comp. Eng., vol. 5, no 2, pp. 398-417, June 2026.

Abstract

The Yeşilyurt Fault (YF) is an approximately 70 km long, NE–SW-trending, left-lateral strike-slip fault located in eastern Türkiye and constitutes a major structural element for assessing regional seismic hazard in Malatya Province. This study integrates multiple morphometric indices to quantitatively evaluate the spatial variability of tectonic activity along the YF and its associated drainage basins. Morphometric analyses were performed using mountain-front sinuosity (Smf), valley floor width–valley height ratio (Vf), hypsometric curves (HC) and hypsometric integrals (HI), asymmetry factor (AF), and stream length–gradient index (SL). These indices were applied to drainage basins distributed along four fault segments (S1–S4) to assess relative tectonic activity, uplift, basin tilting, and landscape evolution. Additionally, empirical fault length–magnitude relationships were used to estimate the seismic potential of individual segments and the entire fault zone. The results indicate that the S1, S2, and S3 segments are characterized by moderate to relatively high tectonic activity, reflected by moderate Smf and Vf values, elevated SL indices, and uplift rates ranging from 0.05 to 0.5 mm/yr. In contrast, the S4 segment exhibits comparatively lower tectonic activity, with uplift rates below 0.05 mm/yr, likely influenced by enhanced erosional processes and extensive alluvial fan development. Hypsometric analyses reveal pronounced spatial variability in basin evolution, ranging from youthful to mature and old geomorphic stages, while AF results indicate that approximately 80% of the drainage basins display asymmetric geometries, suggesting active tectonic tilting. The calculated relative tectonic activity (Iat) indices further confirm that the S1, S2, and S3 segments exhibit high tectonic activity, whereas the S4 segment is characterized by moderate activity. The occurrence of the Mw 6.0 earthquake on 6 October 2024 confirms the present-day activity of the YF, and when integrated with morphometric results and empirical estimates indicating a potential Mw ~7.2 earthquake in the case of full-fault rupture, the YF represents a significant seismic hazard for the region.

Keywords: Earthquake, Malatya, Morphometric analysis, Seismic hazard, Tectonic

*Corresponding author

Plagiarism Checks: Yes – Turnitin
Complaints: fujece@firat.edu.tr

1. Introduction

Earthquake hazard refers to the potential for damage and loss of life resulting from ground motion within a specific region and time period, whereas earthquake risk expresses the probability of physical, economic, and social losses caused by earthquakes [1]. Owing to uncertainties in the location, timing, magnitude, and characteristics of future earthquakes, probabilistic approaches play a key role in earthquake hazard assessment. Numerous studies have been conducted to evaluate earthquake hazard and risk in Türkiye and its surrounding regions and to reduce potential losses, and such investigations are ongoing [2-11]. This study aims to investigate the tectonic geomorphology and deformation characteristics of the Yeşilyurt Fault (YF) using morphometric analyses commonly applied in active tectonic studies. Previous studies on the YF have largely focused on fault kinematics and geometry, with limited attention to morphometric approaches. By examining the tectonic dynamics of individual fault segments, this study seeks to analyze relative tectonic movements and assess the earthquake potential of the region. The specific objectives are to identify the segments of the YF, evaluate their relative tectonic activity using morphometric indices, estimate the maximum earthquake magnitudes the fault segments may generate, and assess the regional seismic hazard potential.

Morphometric analyses employed in this study include Mountain Front Sinuosity (Smf), Valley Floor Width–Valley Height Ratio (Vf), Asymmetry Factor (AF), Stream Length–Gradient Indice (SL), Hypsometric Curve (HC), and Hypsometric Integral (HI). These indices are used to evaluate the effects of tectonic uplift and erosion on valley morphology, the geomorphological maturity of the landscape, basin-scale morphological changes driven by tectonic processes, and the temporal evolution of drainage network deformation related to tilting. In addition, the applied indices provide insights into relative uplift rates through slope-area relationships within the drainage basins.The existence of the Yeşilyurt Fault (YF) has been recognized by numerous researchers and referred to by different names in the literature [12-14]. The YF is a ~70 km long, NE-SW-trending, left-lateral strike-slip fault (Figure 1). It is composed of parallel to sub-parallel fault segments of varying lengths. Along the fault zone, Permian–Triassic metamorphic rocks, Late Cretaceous magmatic rocks, and Middle Eocene units are tectonically juxtaposed with Quaternary basin-fill deposits (Figure 2). The YF has not produced any documented surface-rupturing earthquakes during historical and instrumental periods; nevertheless, the fault zone is characterized by frequent small- to moderate-magnitude seismicity [15-16]. The largest instrumental-period earthquake on the YF occurred on 6 October 2024 with a magnitude of Mw 6.0 and an epicenter in Kale (Malatya); focal mechanism solutions are consistent with strike-slip faulting [16].

Previous studies of the study area focused on the regional stratigraphy, petrography, and geodynamic evolution of the region [12, 17-26, 27]. The most detailed study of the tectonic evolution of the region was carried out by Köküm and İnceöz [23] in the YF. Based on the fault slip data, four successive deformation phases are defined in the study area since early Paleocene. The first deformation phase is characterized by N–S compression during the early Paleocene. The second deformation phase is NW-SE extension related to slab steepening and breakoff in late Paleocene-early Miocene. The third deformation phase is a NNE- SSW compressional one in the middle Miocene-early Pliocene. The fourth and youngest deformation phase is marked by strike-slip faulting under NNE–SSW compression.

2. Geological Background

The Eastern Anatolian Plateau formed at approximately ~12 Ma during the Serravallian as a result of the closure of the Neotethys Ocean and the subsequent collision between the Eurasian and Arabian plates. [28]. Following this collision, continental convergence, crustal thickening, and magmatic activity occurred, and the region became characterized by E–W-trending folds, thrusts, and strike-slip faults [29]. Another consequence of the collision was the formation of the North Anatolian Fault (NAF) and the East Anatolian Fault (EAF) [28-30].

In the study area, different types of rock units ranging from Precambrian to Holocene age are exposed (Figure 2). The closure of the Neotethys Ocean along the Bitlis Suture Zone (BSZ) from the Late Cretaceous to the Middle Miocene, together with the collision between the Arabian and Anatolian plates, played an important role in the emplacement of rocks in the study area [31-32]. The oldest geologic unit in the study area is the Permo–Triassic Keban Metamorphics, which form the basement underlying the Paleozoic, Mesozoic, and Cenozoic rocks and sediments. This unit consists mainly of platform-type carbonate and clastic rocks that have been regionally metamorphosed under greenschist-facies conditions. Late Cretaceous units include the Guleman Ophiolite and the Elazığ Magmatics [33], which are composed predominantly of harzburgite and dunite lenses, and volcanic and plutonic rocks, respectively. The Middle Eocene Maden Complex is represented in the study area mainly by basaltic and andesitic rocks. The Late Miocene–Early Pliocene Çaybağı Formation is characterized by volcanic and sedimentary rocks. The youngest geologic unit in the study area is the Quaternary Palu Formation, which comprises alluvial deposits, travertine, and basaltic rocks that overlie the older units [14, 18-21, 25-34].

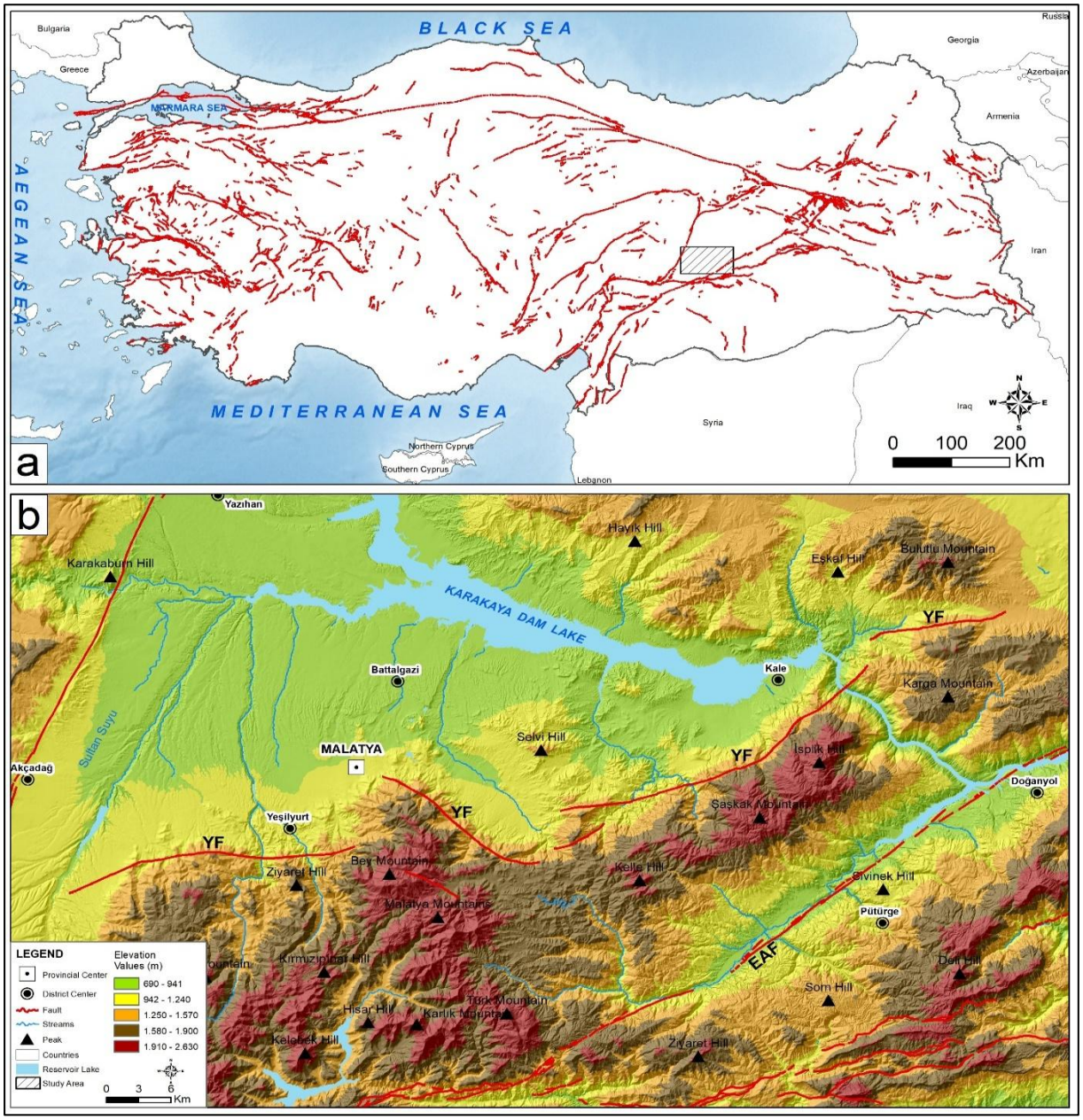

Figure 1. a) Tectonic map of Türkiye showing active faults [35]; (b) location of the Yeşilyurt Fault in the study area

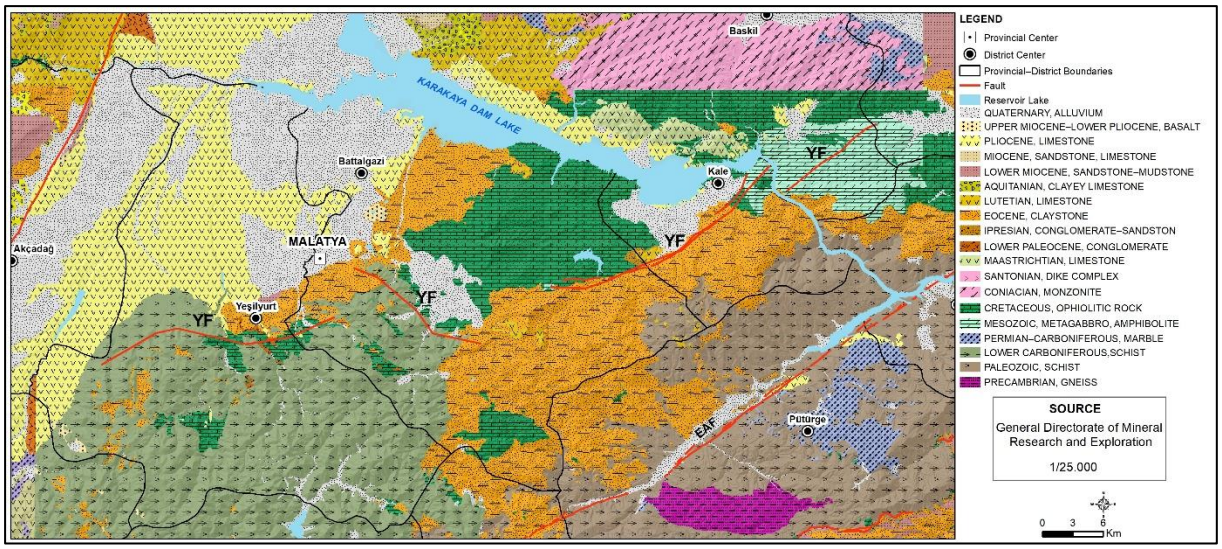

Figure 2. Geological map of the study area [36]

3. Morphometric Analysis

In geomorphology, morphometric analysis involves the quantitative assessment of landforms using mathematical and statistical measurements. Such quantitative approaches enable accurate analysis of landforms and provide valuable information for planning and development purposes. Moreover, morphometric analysis is particularly useful for quantifying landform characteristics of evolutionary significance [37]. By applying geomorphic indices, factors including the linearity or sinuosity of mountain fronts, river flow directions, valley development, and drainage network geometry are systematically analyzed, providing valuable insights into the active tectonic processes shaping the region [37]. In recent years, morphometric analyses have been increasingly supported by digital elevation model (DEM) data and Geographic Information System (GIS) technologies, utilizing digital elevation models, topographic maps, satellite imagery, and GIS platforms such as ArcGIS and QGIS [38-39].

For these analyses, 1:25000-scale topographic maps obtained from the Türkiye Ministry of National Defense and USGS Earth Explorer data with a 10 m–resolution DEM were used. The drainage basins were delineated using the hydrology tool of ArcGIS Pro software.

In A total of 15 drainage basins associated with the Yeşilyurt Fault were analyzed and numbered sequentially from east to west.

3.1. Mountain front sinuosity (Smf)

Mountain-front sinuosity (Smf) is defined as the ratio between the length of a mountain front (Lmf) and its length measured along a straight line (Ls). Mountain-front morphology is directly associated with tectonism. A high degree of sinuosity along mountain fronts indicates that they are strongly affected by erosional processes and therefore represent tectonically inactive mountain fronts. However, tectonically active mountain fronts resist erosional processes and exhibit a linear morphology along mountain slopes [40] (Figure 3).
Mountain-front sinuosity was formulated by Bull as follows [37, 41, 42]

$$Smf = \frac{Lmf}{Ls} \quad (1)$$

Smf, it is the mountain-front sinuosity indices.

Lmf, it is the length of the mountain front at the base of the mountain, that is, the length of the topographic break in slope. **Ls**, it is the length of the mountain front measured along a straight line.

Smf values are generally less than 3. As these values approach 1, they indicate a young geomorphic feature characterized by linearity produced by fault activity. The threshold value for the Smf morphometric indices are commonly accepted as 1.40. Accordingly, Smf values < 1.40 indicate high tectonic activity, whereas Smf values > 1.40 suggest lower tectonic activity [2, 43].

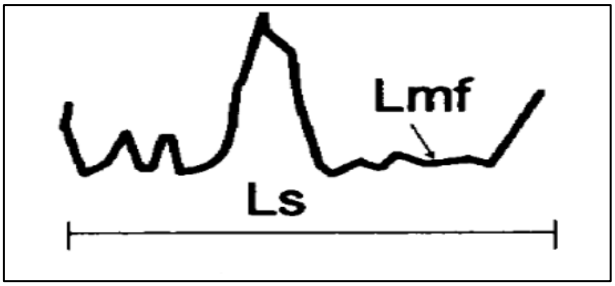

Figure 3. Calculation method of the mountain-front sinuosity (Smf) [44]

3.2. Hypsometric integral (HI) and hypsometric curve (HC)

The hypsometric curve (HC) represents the proportion of the Earth's surface area lying above a given elevation, whereas the hypsometric integral (HI) is a geomorphometric indices used to infer the temporal stages of geomorphic development. The HC is derived from the relationship between relative area and relative elevation within a drainage basin and is expressed by the elevation–area equation. Accordingly, the hypsometric curve provides insights into the evolutionary stage of drainage basins with varying relief and the degree of denudation affecting the landscape. Convex hypsometric curves indicate slightly eroded, youthful basins; S-shaped curves characterize moderately eroded basins in a mature stage; and concave curves represent highly eroded, old basins. The hypsometric integral (HI) is the numerical expression of the hypsometric curve and serves as a quantitative parameter for evaluating topographic evolution within the erosion cycle [45]. HI values generally range between 0.15 and 0.85 and commonly cluster between 0.4 and 0.6. Values of 0.00–0.40 indicate old terrains, values of 0.40–0.60 correspond to mature terrains, and values ≥0.60 represent young topography [46-51] (Figure 4).

$$\mathrm{HI} = \frac{\text{Average Elevation} - \text{Minimum Elevation}}{\text{Maximum Elevation} - \text{Minimum Elevation}} \tag{2}$$

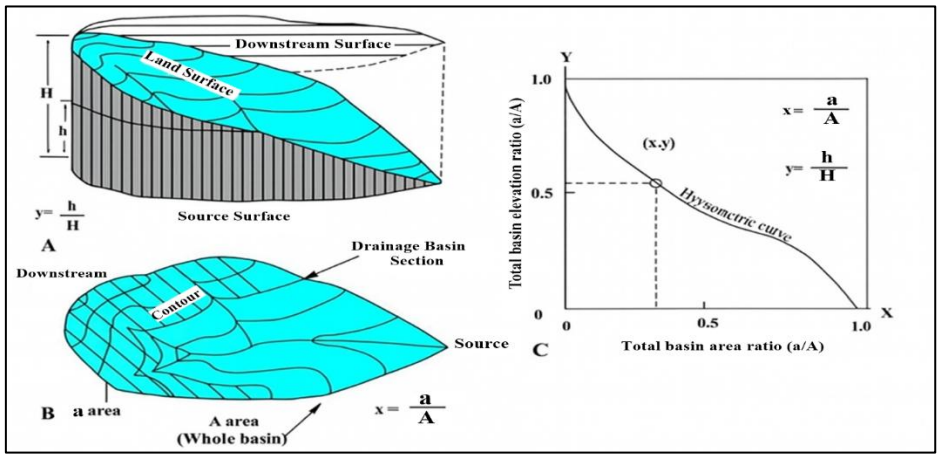

Figure 4. Hypsometric curve (HC) and hypsometric integral (HI) calculation method [2] modified and quoted by [52]

3.3. Valley floor width-valley height ratio (Vf)

The valley floor width–valley height ratio (Vf) is used to distinguish between V-shaped and U-shaped valleys and serves as an indicator of active tectonics [37]. U-shaped valleys may form either through glacial processes or as a result of passive geomorphic evolution. Vf values vary according to valley morphology; therefore, to obtain representative results, measurements should be conducted along river valleys close to mountain fronts. Based on Vf values, valleys are commonly classified into three categories: Class 1 (Vf ≤ 0.5), Class 2 (0.5 < Vf < 1), and Class 3 (Vf ≥ 1) [37, 40, 49, 53-54].

The Vf morphometric indices are commonly calculated using the following equation [37, 40] (Figure 5):

$$Vf = \frac{2V_{fw}}{(E_{ld} - E_{sc}) + (E_{rd} - E_{sc})} \tag{3}$$

where:
Vfw is the valley floor width;
Eld and Erd represent the elevations of the left and right valley divides, respectively;
Esc denotes the elevation of the valley floor.

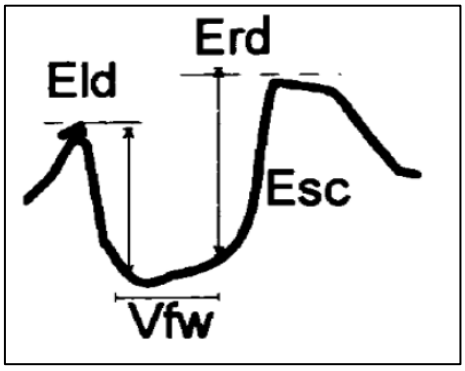

Figure 5. Valley floor - valley height ratio [44]

3.4. Asymmetry factor (AF)

The asymmetry factor (AF) indices are used to evaluate basin tilting within a drainage basin [2]. Moving from the upstream (source) to the downstream (mouth) direction, the AF value is calculated as the ratio of the area located on the right side of the basin's longitudinal axis to the total basin area [49] (Figure 6). The AF indices assesses the degree of basin symmetry and provides insight into the influence of tectonic movements on basin morphology. The drainage basin asymmetry factor is calculated using the following equation:

$$AF = 100\frac{Ar}{At} \tag{4}$$

where Ar represents the area on the right side of the drainage basin, and At denotes the total drainage basin area. An AF value close to 50 indicates a symmetrical basin with no significant tilting, suggesting minimal or no tectonic influence. In contrast, AF values significantly deviating from 50 (i.e., AF < 45 or AF > 55) indicate basin tilting, implying the influence of tectonic activity. Based on the degree of deviation from symmetry, drainage basins are commonly classified into three categories [43, 48], as summarized in Table 1.

Table 1. Classification of drainage basin asymmetry based on the AF indices

Grade	Value Range	Description
Low Asymmetry	AF ≈ 50	Indicates a nearly symmetrical drainage basin with no significant tectonic influence.
Moderate Asymmetry	AF = 45-55	Indicates slight basin asymmetry, suggesting possible tectonic influence.
High Asymmetry	AF <45 or AF> 55	Indicates pronounced basin asymmetry, reflecting strong tectonic control on basin morphology.

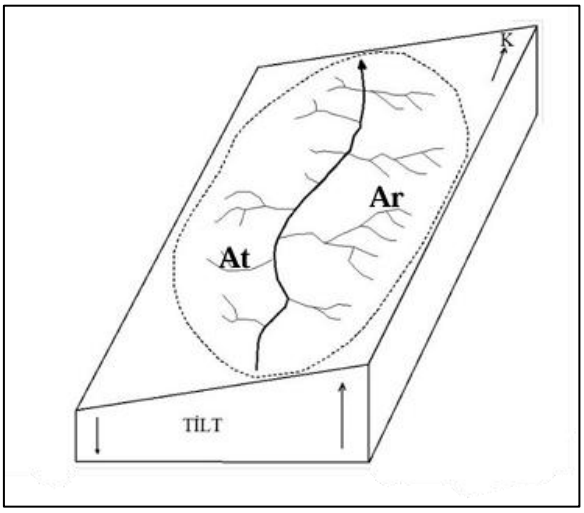

Figure 6. Drainage basin asymmetry block diagram [2]

3.5. Stream length-gradient (SL)

The stream length-gradient (SL) indices are a widely used geomorphic parameter for assessing active tectonic processes and regional deformation by examining variations in channel slope along a river's longitudinal profile. The SL indices are designed to identify slope anomalies along stream channels, which are commonly associated with tectonic activity, lithological contrasts, or climatic influences. Hack [55] first defined the SL indices as "the product of the slope of a given reach of a stream channel and the total channel length from the drainage divide to the midpoint of that reach" (Figure 7).
The SL indices are mathematically expressed as:

$$SL=(\Delta H/\Delta L)*L \quad (5)$$

where:
ΔH is the elevation difference along the selected stream segment;
ΔL is the length of the stream segment;
L is the channel length measured from the midpoint of the stream segment to the upstream drainage divide of the basin.

High SL values generally reflect active tectonic deformation, erosion-resistant lithologies, and the presence of knickpoints associated with abrupt slope changes along river longitudinal profiles.

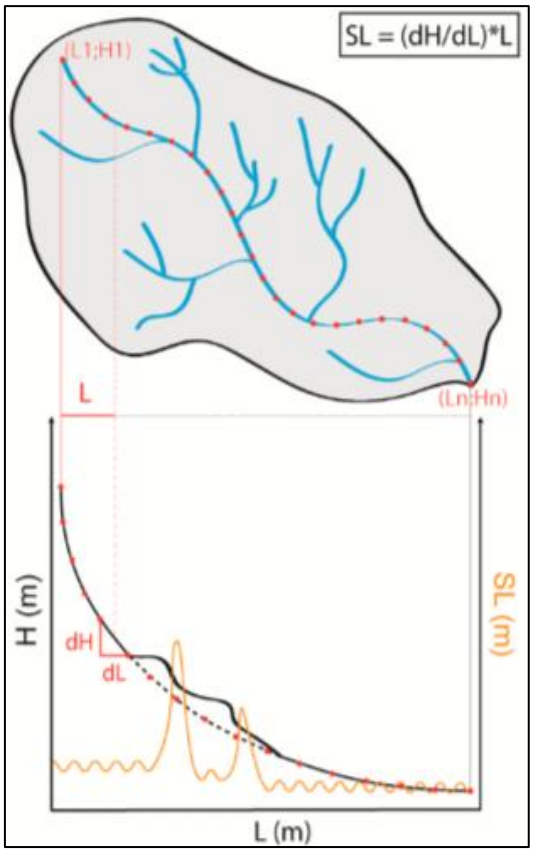

Figure 7. Calculation of SL values along the flow following the Hack equation [56]

4. Results

4.1. Mountain front sinuosity (Smf)

Mountain-front sinuosity (Smf) values were calculated to assess the relative tectonic activity along the mountain fronts controlled by the Yeşilyurt Fault segments. Smf measurements were calculated at four different sites along the fault (Figure 8). The calculated Smf values range between 1.70 and 3.50. The lowest Smf value (1.73) was obtained for the S3 segment, whereas the highest value (3.41) was calculated for the S4 segment, located in the westernmost part of the fault (Table 2).

Table 2. Smf values of the Yeşilyurt Fault segments

Segment number	Lmf	Ls	Smf
S1	22512	10657	2.11
S2	48054	24642	1.95
S3	24463	14079	1.73
S4	70014	20518	3.41

Low Smf values indicate active uplift, whereas high Smf values suggest reduced tectonic activity and dominant erosional processes [57-58]. Four distinct mountain fronts were identified across the 15 drainage basins. The lowest Smf value was obtained for the S3 segment, indicating active tectonism, whereas the highest Smf value was calculated for the S4 segment, which is located in the westernmost part of the fault. The S1, S2, and S3 segments fall into Class 2 ($1.4 \leq Smf < 3.0$), corresponding to moderate tectonic activity, while the S4 segment belongs to Class 3 ($Smf \geq 3.0$), indicating low tectonic activity.Following the classification proposed by El Hamdouni et al. (2008)

[38], Smf values were grouped into three classes: Class 1 (Smf < 1.4) corresponds to high tectonic activity, Class 2 (1.4 ≤ Smf < 3.0) corresponds to moderate tectonic activity, and Class 3 (Smf ≥ 3.0) corresponds to low tectonic activity.

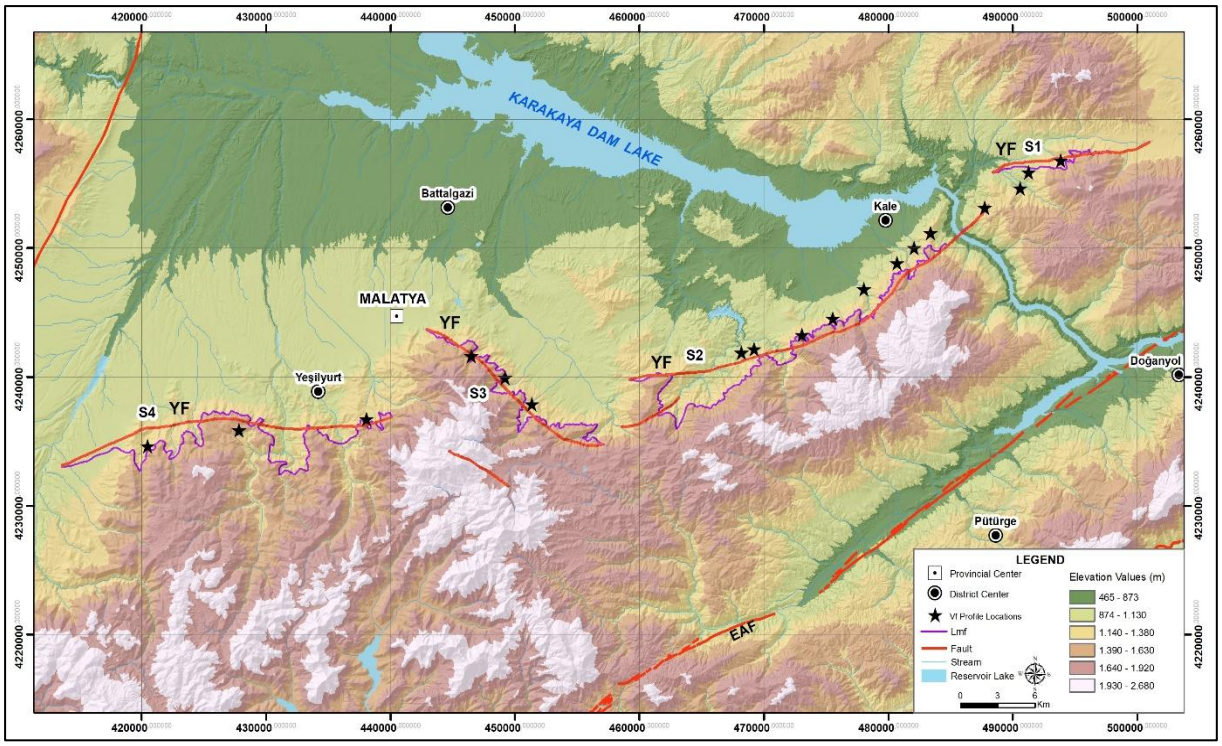

Figure 8. Locations of mountain-front sinuosity (Smf) and valley floor width-valley height ratio (Vf) measurements in the study area

4.2. Hypsometric integral (HI) and hypsometric curve (HC)

Hypsometric integral (HI) values were calculated for 15 drainage basins using DEM data, and the corresponding hypsometric curves (HC) were generated (Figures 9 and 10). The HC graphs were produced using the CalHypso plugin. The HI values of the drainage basins range between 0.33 and 0.68. As shown in Figure 9, green-colored basins represent young basins (HI > 0.6), yellow-colored basins indicate mature basins (0.35 < HI < 0.6), and brown-colored basins represent old basins (HI < 0.35).

Drainage basin no. 4, which has the highest HI value (0.67), represents a young basin, whereas drainage basin no. 12, with the lowest HI value (0.31), corresponds to a relatively old basin. Drainage basins with HI values between 0.50 and 0.67 exhibit convex hypsometric curves, indicating limited erosion. Basins characterized by S-shaped hypsometric curves display HI values ranging between 0.30 and 0.49, reflecting a moderate degree of denudation. In contrast, basins with concave hypsometric curves show HI values between 0.35 and 0.42, indicating advanced erosion stages.

Following the classification proposed by El Hamdouni et al. (2008) [38], HI values were grouped into three classes: Class 1 (HI ≥ 0.5) corresponds to convex hypsometric curves, Class 2 (0.4 < HI < 0.5) represents flat S-shaped curves, and Class 3 (HI ≤ 0.4) corresponds to concave hypsometric curves. Overall, the hypsometric curve distribution consists of 26.6% convex, 53.3% flat S-shaped, and 20.1% concave.

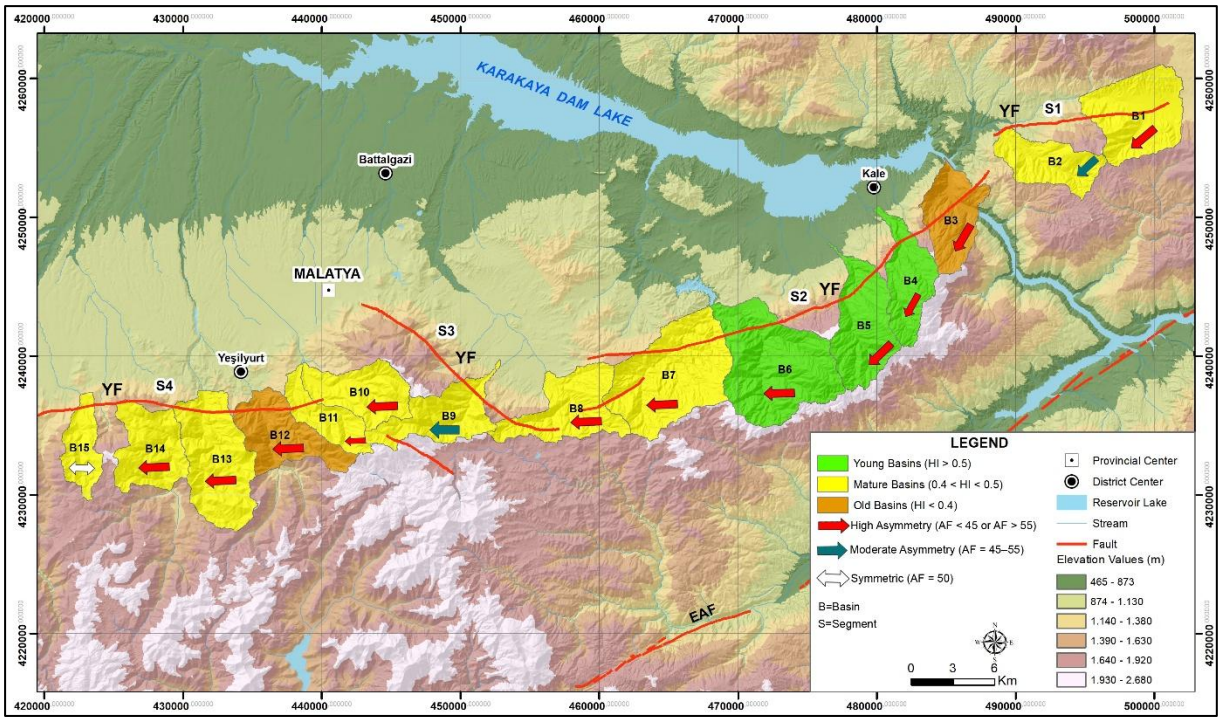

Figure 9. Locations of Hypsometric integral (HI) and asymmetry factor (AF) indices along the Yeşilyurt Fault

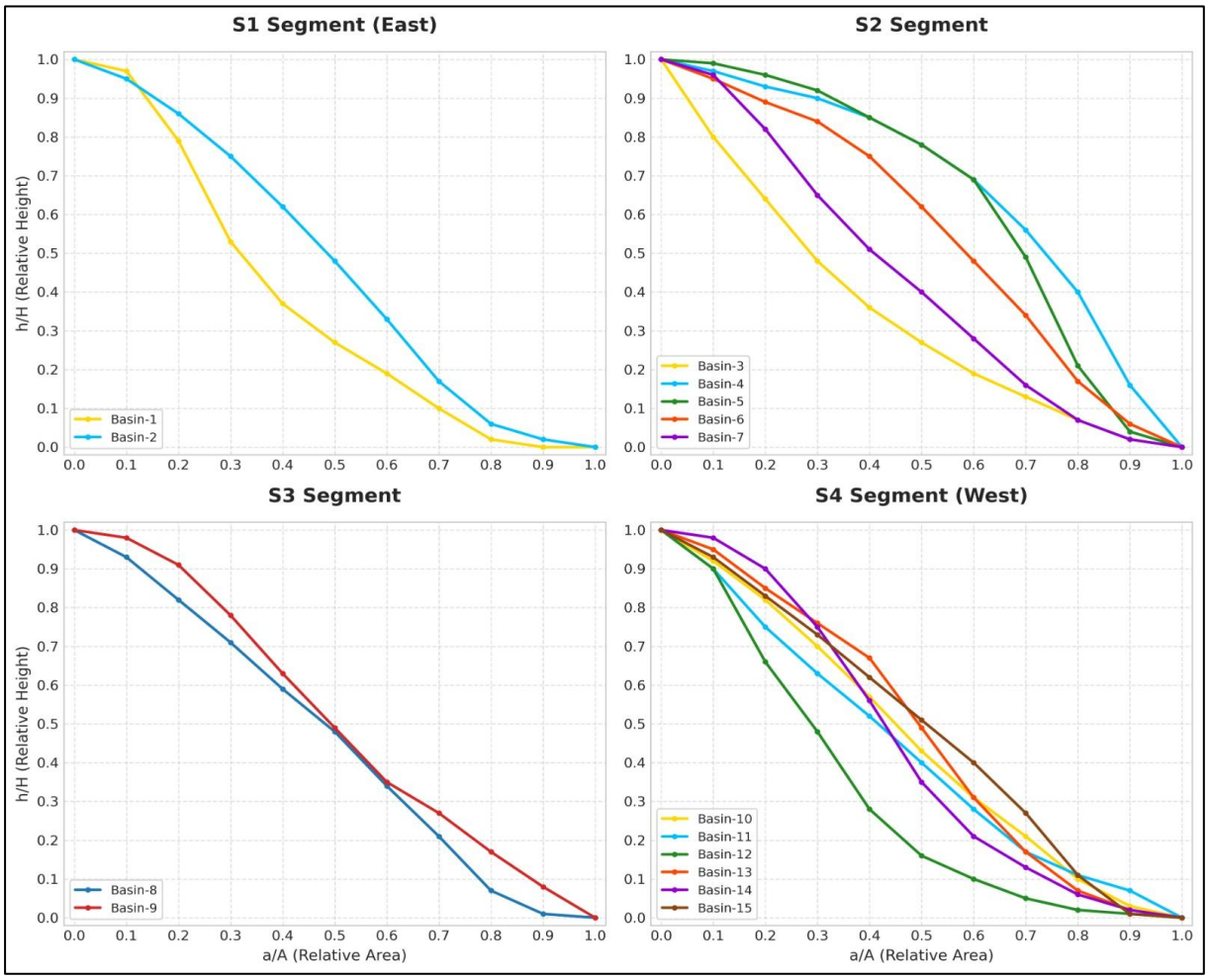

Figure 10. Hypsometric curves (HC) of the S1, S2, S3, and S4 segments

4.3. Valley floor width valley height ratio (Vf)

Valley floor width-valley height ratio (Vf) values were calculated for 15 drainage basins to evaluate relative tectonic uplift rates in the study area. Vf measurements were performed along valley sections located 250 to 500 m upstream from the mountain front, depending on the size of each drainage basin. The calculated Vf values range from 0.28 to 1.81. Following the classification proposed by El Hamdouni et al. (2008) [38], Vf values were grouped into three classes: Class 1 (Vf $\leq$ 0.5) indicates high tectonic activity, Class 2 (0.5 < Vf < 1.0) represents moderate tectonic activity, and Class 3 (Vf $\geq$ 1.0) corresponds to low tectonic activity.

4.4. Asymmetry factor (AF)

The asymmetry factor (AF) indices were calculated for all 15 drainage basins in the study area (Figure 9). The calculated AF values range from 28.60 to 71.06, indicating varying degrees of basin asymmetry across the study area. The lowest AF value (28.60) was obtained for drainage basin no. 21, whereas the highest AF value (71.06) was calculated for drainage basin no. 4. The results indicate that 80% of the drainage basins exhibit asymmetrical basin patterns, while 20% display nearly symmetrical basin characteristics. Following the classification proposed by El Hamdouni et al. (2008) [38], AF values were grouped into three classes: Class 1 (AF <35 or AF> 65) corresponds to high tectonic activity, Class 2 (AF = 35-45 or AF = 55-65) corresponds to moderate tectonic activity, and Class 3 (AF = 45-55) corresponds to low tectonic activity.

4.5. Stream length-gradient (SL)

The stream length-gradient (SL) indices are calculated for all 15 drainage basins (Figure 11). The calculated SL values range from 198.05 to 914.38. Following the classification proposed by El Hamdouni et al. (2008) [38], SL values were grouped into three classes: Class 1 (SL> 500) corresponds to high tectonic activity, Class 2 (250 < SL < 500) corresponds to moderate tectonic activity. Class 3 (SL < 250) corresponds to low tectonic activity. The results indicate that 40% of the SL indices values correspond to high tectonic activity (Class 1), 46.6% correspond to moderate tectonic activity (Class 2), and the remaining 13.3% reflect low tectonic activity (Class 3) characteristics (Figure 14).

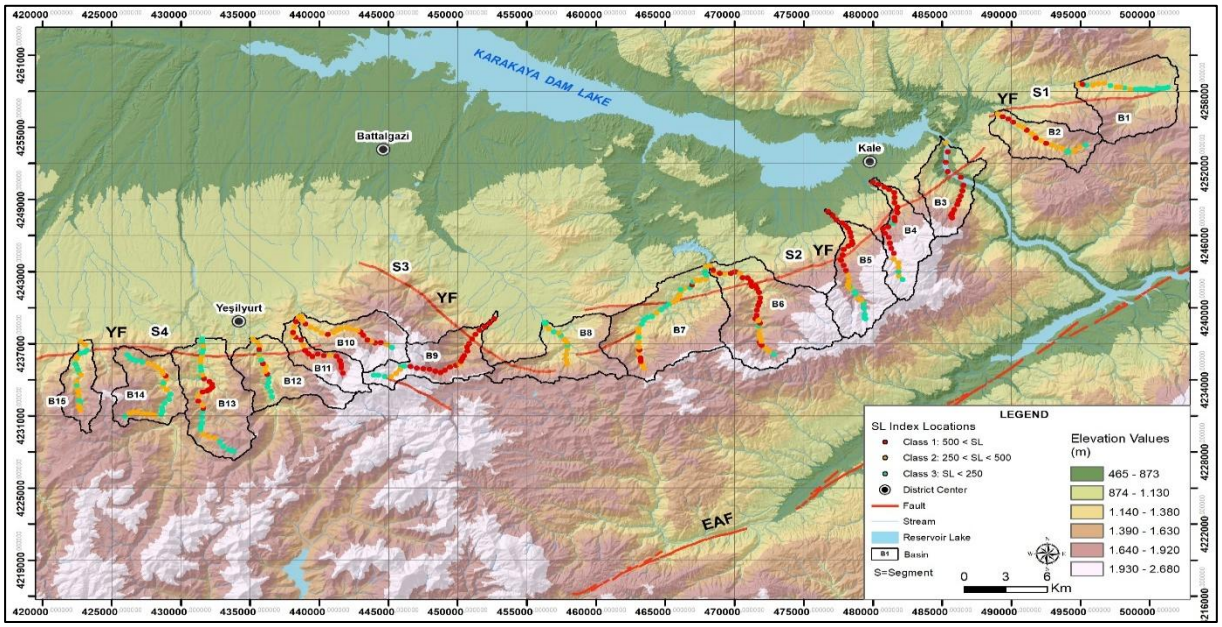

Figure 11. Locations of stream length–gradient (SL) indices along the Yeşilyurt Fault

4.6. Yeşilyurt Fault Earthquake Magnitude Calculations

The Yeşilyurt Fault (YF) is a potentially active fault zone approximately 70 km in length, trending east-northeast (ENE) and characterized by left-lateral strike-slip motion. It represents one of the major structural elements with a high potential to affect the Malatya Province [22].

Following the empirical relationships proposed by Wells and Coppersmith (1994) [59], the potential earthquake magnitudes that could be generated by individual fault segments as well as by the entire fault system were estimated based on fault length. The relevant equations are as follows:

$$M=a+b*\log(SRL) \quad (6)$$

$$M_w=5{,}16+(1{,}12 \times \log(L)) \text{ (for strike-slip faults)} \quad (7)$$

where, M_w is the moment magnitude, and L is the length of a strike slip fault.
Based on these equations, the estimated moment magnitudes for the Yeşilyurt Fault segments are:

S1 segment (L = 10 km): M_w= 6.3
S2 segment (L = 24 km): M_w= 6.7
S3 segment (L = 14 km): M_w= 6.4
S4 segment (L = 20 km): M_w= 6.6

Considering the rupture of the entire fault length (L = 70 km), the maximum expected earthquake magnitude is estimated to be approximately M_w = 7.2, (Figure 12).

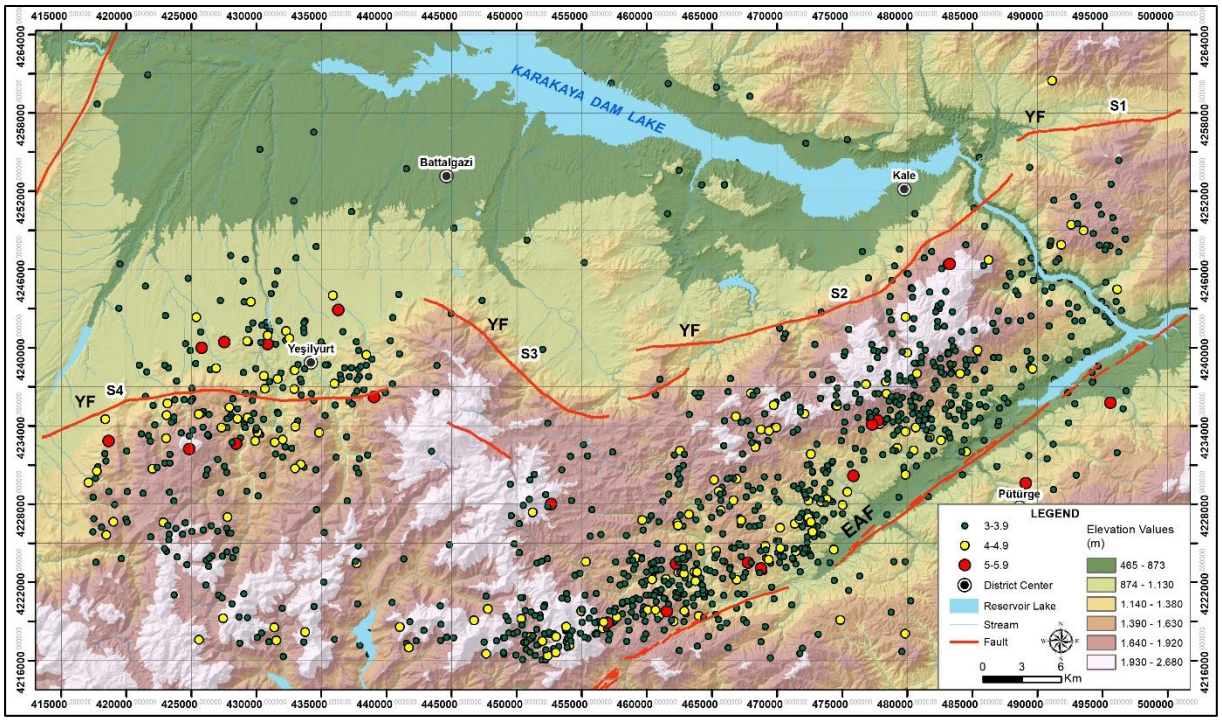

Figure 12. Spatial distribution of earthquakes with Mw ≥ 3.0 along the Yeşilyurt Fault (1900–2024)

5. Discussion

Morphometry has become a widely used method in active tectonic studies in recent years, and it is frequently applied in morphometry-based research conducted at both national and international scales. Mountain-front sinuosity (Smf) is defined as the ratio between the length of a mountain front (Lmf) and its length measured along a straight line (Ls). In general, low Smf values indicate young and tectonically active mountain fronts characterized by linear morphologies, whereas higher values

reflect reduced tectonic activity and increased modification by erosional processes. Accordingly, the S1, S2, and S3 segments, which display moderate Smf values, indicate moderate to relatively high tectonic activity (Table 2 and 3). In contrast, the S4 segment, with an Smf value greater than 3, suggests a lower degree of tectonic activity.

Table 3. Morphometric indices and classification of drainage basins in the study area

Drainage number		Area (km^2)	HI		Smf		Vf		Af		SL		lat
			Value	Class	Value	Class	Value	Class	Value	Class	Value	Class	
S1	1	36.38	0.37	3	2.11	2	0.4	1	33.11	1	198.05	3	2-H
	2	21.85	0.47	2		2	1.05	3	46.67	2	407.68	2	3-M
S2	3	23.91	0.34	3	1.95	2	0.28	1	44.03	1	898.89	1	2-H
	4	22.85	0.67	1		2	0.85	2	71.06	1	914.38	1	1-VH
	5	31.70	0.64	1		2	0.69	2	60.66	1	712.64	1	1-VH
	6	54.97	0.56	1		2	0.4	1	62.85	1	590.80	1	1-VH
	7	52.68	0.43	2		2	0.2	1	62.57	1	314.83	2	2-H
	8	30.35	0.46	2		2	0.5	1	56.46	1	263.70	2	2-H
S3	9	25.68	0.51	2	1.73	2	0.61	2	54.23	2	643.08	1	2-H
S4	10	24.35	0.46	2	3.41	3	0.38	1	43.35	1	484.54	2	2-H
	11	15.90	0.43	2		3	0.53	2	37.83	1	561.48	1	2-H
	12	27.45	0.31	3		3	0.4	1	28.60	1	274.15	2	3-M
	13	40.74	0.47	2		3	1.81	3	64.04	1	347.81	2	3-M
	14	26.03	0.45	2		3	1.11	3	34.99	1	259.65	2	3-M
	15	14.56	0.48	2		3	0.62	2	53.42	3	243.61	3	4-L

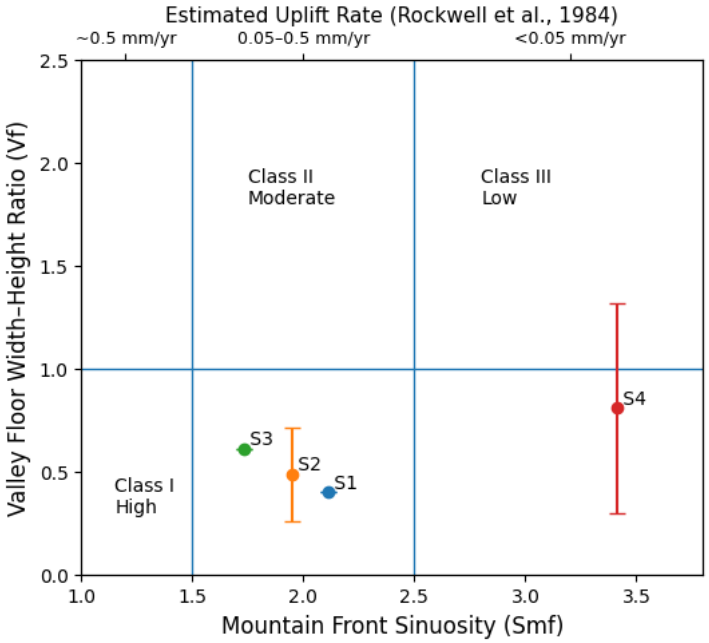

Figure 13. Smf–Vf plot showing relative tectonic activity classes and estimated uplift rates [59] for the Yeşilyurt Fault segments. Points represent segment mean values with standard deviation

Low and moderate Smf values are indicative of mountain fronts under strong tectonic influence and imply that the region is affected by active tectonism [38]. The relatively high Smf value calculated for the S4 segment (3.41) is likely related to the disruption of mountain-front linearity by slope debris accumulation and the development of alluvial fans in front of the fault.

The hypsometric curve provides insights into the evolutionary stage of drainage basins with varying relief and the degree of denudation affecting the landscape. Low HI values for basins 1, 3, and 12 indicate mature stages and low tectonic activity, whereas the remaining basins exhibit moderate to high tectonic activity (Table 3). As shown in Figure 9, green-colored basins represent young basins, yellow-colored basins indicate mature basins, and brown-colored basins represent old basins.

Drainage basin no. 4, which has the highest HI value (0.67), represents a young basin, whereas drainage basin no. 12, with the lowest HI value (0.31), corresponds to a relatively old basin. Drainage basins with HI values between 0.50 and 0.67 exhibit convex hypsometric curves, indicating limited erosion. Basins characterized by S-shaped hypsometric curves display HI values ranging between 0.30 and 0.49, reflecting a moderate degree of denudation. In contrast, basins with concave hypsometric curves show HI values between 0.35 and 0.42, indicating advanced erosion stages.

The valley floor width–valley height ratio (Vf) is used to distinguish between V-shaped and U-shaped valleys and serves as an indicator of active tectonics. Low Vf values indicate the development of V-shaped valleys associated with high tectonic activity, whereas high Vf values correspond to U-shaped valleys and reflect low tectonic activity [37, 40, 49, 53–54]. High Vf values for basins 1, 3, and 12 indicate mature stages and low tectonic activity, while the remaining basins exhibit moderate to high tectonic activity (Table 3).

The combined use of the Smf and Vf indices allows the interpretation of relative tectonic activity and the estimation of uplift rates [59]. For the YF segments, the calculated uplift rates range from 0.05 to 0.5 mm/yr for the S1, S2, and S3 segments, whereas the uplift rate for the S4 segment is lower than 0.05 mm/yr (Figure 13).

The asymmetry factor (AF) index is used to evaluate basin tilting within drainage basins [2]. The results indicate that 80% of the drainage basins exhibit asymmetric basin patterns, whereas 20% display nearly symmetrical basin characteristics.

The stream length–gradient (SL) index is used to identify slope anomalies along stream channels, which are commonly associated with tectonic activity, lithological contrasts, or climatic influences [55]. The calculated SL values range from 198.05 to 914.38. The results indicate that 86.6% of the SL index values correspond to moderate to high tectonic activity, whereas the remaining 13.3% reflect low tectonic activity characteristics.

In addition, the mean values of the morphometric indices (HI, Smf, Vf, AF, and SL) were used to calculate the relative tectonic activity index (Iat) following the classification proposed by El Hamdouni et al. (2008). This scheme divides relative tectonic activity into four classes: very high ($1.0 < Iat < 1.5$), high ($1.5 \leq Iat < 2.0$), moderate ($2.0 \leq Iat < 2.5$), and low ($Iat \geq 2.5$) (Table 3). The resulting Iat values indicate marked spatial variability among the analyzed drainage basins. Basins 4, 5, and 6 within Segment S2 exhibit very high tectonic activity. High activity characterizes basins 1 (S1), 3, 7, and 8 (S2), 9 (S3), and 10 and 11 (S4). Basins 2 (S1) and 12, 13, and 14 (S4) are classified as moderate, whereas only basin 15 (S4) corresponds to the low activity class. Notably, all basins in Segment S2 fall within the very high and high categories. In contrast, Segment S4 shows a wider distribution, with 50% of its basins classified as high, 37.5% as moderate, and 12.5% as low.

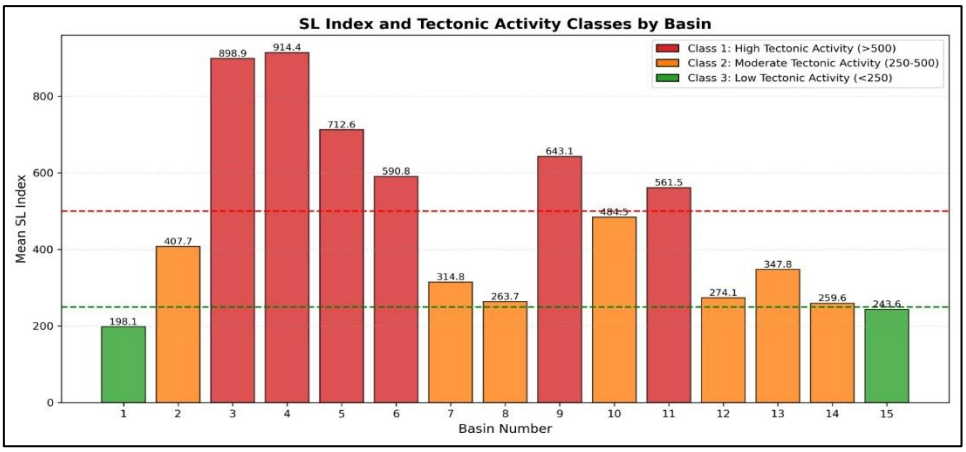

Figure 14. SL indices and tectonic activity classes by basin

Previous studies have demonstrated that morphometric analyses are effectively applicable to active fault zones and provide valuable insights into tectonic activity (e.g., [3, 7, 11, 17, 46, 50, 60, 61]). A recent morphometry-based study on the Kale–Yeşilyurt Fault published by Akgün [17] suggested that the Kale Fault, representing the eastern part of the deformation zone, exhibits a dominant normal faulting component, whereas the Yeşilyurt Fault to the west is relatively more tectonically active. The study further indicates that active tectonic processes continue along both fault segments. Despite focusing on the same fault zone, there are notable methodological and structural differences between Akgün's study and the present work. Differences in fault geometry interpretation, the variety of morphometric indices employed, and the number of drainage basins or drainage networks included in the analyses limit the direct comparability of the results. These methodological differences particularly affect the evaluation of morphometric parameters at the segment scale and necessitate a re-examination of the spatial distribution of tectonic activity along the fault zone. Nevertheless, the findings of both studies consistently indicate that the Yeşilyurt Fault is characterized by low to moderate tectonic activity.

Morphometric approaches have also been widely applied to other major fault systems in Türkiye. Khalifa et al. [60] investigated the East Anatolian Fault (EAF) using digital elevation models and applied several morphometric indices, including the stream length–gradient index (SL), mountain-front sinuosity (Smf), valley floor width–valley height ratio (Vf), basin asymmetry factor (AF), drainage density, and hypsometric analysis. Based on tectonic geomorphological characteristics, the EAF was divided into five main segments, along which SL values range between 50 and 350. Similarly, Zabcı [11] applied hypsometric curves and integrals, normalized steepness and concavity, and longitudinal profile analyses to 27 drainage basins distributed along five segments of the Malatya Fault (MF). That study revealed distinct variations in tectonic activity among the segments, with high activity along FS1, moderate activity along FS2 and FS3, and a balance between tectonic and erosional processes along FS4 and FS5. Balkaya [3] conducted a morphometric study on the Yesemek Segment of the Ölüdeniz Fault (ÖDF), calculating Smf, Vf, AF, hypsometric curves (HC) and integrals (HI), and the SL index, and identified moderate to high tectonic activity across different parts of the segment. Similarly, Mutlu [61] applied morphometric analyses, including surface roughness, hypsometric integral, basin asymmetry factor, mountain-front sinuosity, and the valley floor width–valley height ratio, to the Iğdır Fault Zone (IFZ) within the Lesser Caucasus Tectonic Block. The results indicated the presence of a normal faulting component, uplift rates exceeding 0.5 mm/yr in the northwestern and southeastern sections, and increased deformation accumulation in the southeastern segments near Mount Ağrı. Overall, these studies demonstrate that morphometric indices applied in different tectonic settings provide robust information on deformation characteristics and relative tectonic activity levels of fault zones. Analyses conducted on different sections of the same fault consistently reveal significant along-strike variations in tectonic activity. Within this framework, the results of the present study indicate that the Yeşilyurt Fault exhibits relatively lower tectonic activity compared to the EAF and the ÖDF, and that the

application of similar morphometric indices to different fault systems yields results consistent with their relative tectonic activity levels. The seismic potential of the Yeşilyurt Fault is further emphasized by the occurrence of the largest instrumental-period earthquake on the fault, which took place on 6 October 2024 with a magnitude of Mw 6.0 and an epicenter near Kale (Malatya). The focal mechanism solutions indicate dominant strike-slip faulting, consistent with the kinematic characteristics of the YF. This recent event demonstrates that the fault is currently active and capable of generating damaging earthquakes. When combined with the morphometric indices and empirical magnitude estimates, which suggest that a full rupture of the fault could produce an earthquake of up to Mw 7.2, the Yeşilyurt Fault represents a significant seismic hazard for Malatya Province and its surroundings. These findings highlight the urgent need for detailed paleoseismological investigations and improved seismic hazard assessments in the region.

6. Conclusions

The following conclusions were obtained from this study:

- Integrated morphometric analyses (Smf, HI, Vf, AF, and SL) highlight the important role of the Yeşilyurt Fault in controlling drainage-basin geomorphology.
- The S1, S2, and S3 segments showmoderate to relatively high tectonic activity and uplift rates (0.05–0.5 mm/yr), whereas the S4 segment shows lower tectonic activity with uplift rates below 0.05 mm/yr.
- Hypsometric and Vf analyses of drainage basins reveal that several drainage basins are in mature to old evolutionary stages, while others reflect ongoing tectonic influence, highlighting along-strike variability in landscape evolution.
- SL index results indicate that most drainage basins are affected by moderate to high tectonic activity, supporting active deformation along the fault.
- The Mw 6.0 earthquake of 6 October 2024 confirms the present-day activity of the Yeşilyurt Fault, and empirical estimates suggest that a full rupture could generate an earthquake of up to Mw ~7.2, representing a significant seismic hazard for Malatya Province.

7. Acknowledgement

This article was derived from the MSc thesis entitled ″Determination of the Relative Tectonic Evolution of the Yeşilyurt Fault Using Morphometric Indices″ completed by Selin Salman at the Department of Emergency and Disaster Management, Institute of Graduate Studies, Bitlis Eren University, under the supervision of Dr. Fikri Akgün and co-supervision of Dr. Mehmet Köküm (September 2024). The manuscript has been substantially revised and expanded beyond the original thesis through the application of additional analytical methods, further interpretation of the results, and significant scientific contributions from the co-authors.

8. Author Contribution Statement

All authors contributed equally to this work.

9. Ethics Committee Approval and Conflict of Interest

“There is no conflict of interest with any person/institution in the prepared article. Additionally, ethics committee approval is not required for this study.”

10. Ethical Statement Regarding the Use of Artificial Intelligence

During the preparation of this manuscript, the artificial intelligence tool ChatGPT, developed by OpenAI, was used solely for linguistic editing and translation purposes. All scientific content, analyses, interpretations, and conclusions are the sole responsibility of the authors.

11. References

[1]AFAD, "Deprem nedir?," AFAD Türkiye. [Online]. Available: https://www.afad.gov.tr/kurumlar/afad.gov.tr/39500/xfiles/deprem_nedir.pdf. Accessed: Nov. 20, 2025.

[2] E. A. Keller and N. Pinter, *Active Tectonics: Earthquakes, Uplift, and Landscapes*. Upper Saddle River, NJ, USA: Prentice Hall, 1996. [Online]. Available: http://sutlib2.sut.ac.th/sut_contents/H49253.pdf. Accessed: Nov. 22, 2025.

[3] M. Balkaya, "Ölü Deniz Fay Zonu Yesemek Segmenti'nin morfometrik analiz yöntemleriyle araştırılması," *Erciyes Üniv. Fen Bil. Enst. Fen Bil. Derg.*, vol. 41, no. 1, pp. 370–383, 2025.

[4] M. Bozdoğan and E. Canpolat, "Drenaj havzalarındaki morfotektonik özelliklerin jeomorfik analizlerle incelenmesi: Delibekirli (Kırıkhan/Hatay) Havzası örneği," *Jeomorfolojik Araştırmalar Derg.*, no. 11, pp. 22–51, Oct. 2023.

[5] M. Edemen, "Deprem nedir? Nasıl oluşur? Türkiye'de oluşmuş depremler ve etkileri nelerdir? Depremlere karşı alınabilecek tedbirler hususunda öneriler," *J. Soc. Humanit. Sci. Res.*, p. 93, Jan. 2023.

[6] F. N. Genç, "Türkiye'de doğal afetler ve doğal afetlerde risk yönetimi," *Stratejik Araştırmalar Derg.*, vol. 9, no. 5, pp. 201–226, 2007.

[7] S. Gürgöze and A. Uzun, "Tektoniğin drenaj havzalarına etkisinin morfometrik indislerle incelenmesi, Kuzey Anadolu Fay Zonu'nun Kızılırmak ile Tersakan Çayı arası, Samsun," *Coğrafi Bil. Derg.*, vol. 23, no. 1, pp. 151–178, 2025.

[8] İ. Ketin, "Türkiye'nin genel tektonik durumu ile başlıca deprem bölgeleri arasındaki ilişkiler," *Bull. Miner. Res. Explor.*, vol. 71, no. 71, pp. 129–135, 1968.

[9] İ. Ketin, "Kuzey Anadolu fayı hakkında," *Bull. Miner. Res. Explor.*, vol. 72, no. 72, pp. 1–27, 1969.

[10] Y. Öztürk and H. Zorer, "Neotektonik transfer zonlarında dağlık alanların morfotektonik evrimi: Güneydoğu Anadolu Bindirme Kuşağı'nda Körkandil Dağı örneği (Pervari/Siirt)," *Ege Coğrafya Derg.*, vol. 33, no. 1, pp. 121–142, Jun. 2024.

[11] C. Zabci, "Malatya Fayı'nın morfometrik özellikleri," *Türk Coğrafya Derg.*, no. 75, pp. 107–118, 2020.

[12] N. Kaymakci, M. Inceoez, and P. Ertepinar, "3D-architecture and Neogene evolution of the Malatya Basin: Inferences for the kinematics of the Malatya and Ovacık fault zones," *Turkish J. Earth Sci.*, vol. 15, no. 2, pp. 123–154, 2006.

[13] M. Palutoğlu and E. Tanyolu, "Elazığ il merkezi yerleşim alanının depremselliği," *Fırat Üniv. Fen Müh. Bil. Derg.*, vol. 18, no. 4, pp. 577–588, 2006.

[14] D. Perinçek, *The Geology of Hazro–Korudağ–Çüngüş–Maden–Ergani–Hazar–Elazığ–Malatya Area: Guide Book*. Ankara, Türkiye: TJK Yayını, 1979.

[15] M. Köküm and F. Özçelik, "An example study on re-evaluation of historical earthquakes: 1789 Palu (Elazığ) earthquake, Eastern Anatolia, Turkey," *Bull. Miner. Res. Explor.*, vol. 161, no. 161, pp. 157–170, 2020.

[16] Boğaziçi Üniversitesi Kandilli Rasathanesi ve Deprem Araştırma Enstitüsü, "ZEQDB: Kandilli Rasathanesi Deprem Veritabanı," Kandilli Rasathanesi ve Deprem Araştırma Enstitüsü (KOERI). [Online]. Available: http://www.koeri.boun.edu.tr/sismo/zeqdb/. Accessed: Nov. 22, 2025.

[17] E. Akgün, "Kinematic and morphometric evidence for recent reactivation of the Kale-Yeşilyurt fault zone within the East Anatolian Fault System," *J. Mt. Sci.*, vol. 21, no. 12, pp. 4149–4176, 2024.

[18] M. A. Ertürk, A. Sar, and M. E. Rizeli, "Petrology, zircon U–Pb geochronology and tectonic implications of the A1-type intrusions: Keban region, eastern Turkey," *Geochemistry*, vol. 82, no. 3, Art. no. 125882, 2022.

[19] M. Köküm, "Doğu Anadolu Fay Sistemi'nin Palu-Uslu (Elazığ) arasındaki kesiminin kinematik analizi," Ph.D. dissertation, Fen Bilimleri Enstitüsü, Fırat Üniv., Elazığ, Türkiye, 2017.

[20] M. Köküm, "Landsat TM görüntüleri üzerinden Doğu Anadolu Fay Sistemi'nin Palu (Elazığ)-Pütürge (Malatya) arasındaki bölümünün çizgisellik analizi," *Gümüşhane Üniv. Fen Bil. Enst. Derg.*, vol. 9, no. 1, pp. 119–127, 2019.

[21] M. Köküm, "Kinematic and dynamic fault slip analyses: Implications from the surface rupture of the 2023 Elbistan (Kahramanmaraş) (Mw 7.6) earthquake, Türkiye," *J. Struct. Geol.*, vol. 187, Art. no. 105235, 2024.
[22] M. Köküm and M. İnceöz, "Yeşilyurt-Elazığ fay zonunun yapısal özellikleri," in *Aktif Tektonik Araştırma Grubu 22. Çalıştayı (ATAG-22)*, Çanakkale, Türkiye, Nov. 2018.
[23] M. Köküm and M. İnceöz, "Paleostress analysis of the Yeşilyurt-Elazığ Fault Zone and its importance for the tectonic evolution, East Turkey," *J. Struct. Geol.*, vol. 138, Art. no. 104093, 2020.
[24] A. Sar, M. A. Ertürk, and M. E. Rizeli, "Genesis of Late Cretaceous intra-oceanic arc intrusions in the Pertek area of Tunceli Province, eastern Turkey, and implications for the geodynamic evolution of the southern Neo-Tethys: Results of zircon U–Pb geochronology and geochemical and Sr–Nd isotopic analyses," *Lithos*, vol. 350, Art. no. 105263, 2019.
[25] U. K. Tekin, M. Ural, M. C. Göncüoğlu, M. Arslan, and S. Kürüm, "Upper Cretaceous Radiolarian ages from an arc–back-arc within the Yüksekova Complex in the southern Neotethys mélange, SE Turkey," *C. R. Palevol*, vol. 14, no. 2, pp. 73–84, 2015.
[26] M. Ural, M. Arslan, M. C. Göncüoğlu, K. U. Tekin, and S. Kürüm, "Late Cretaceous arc and back-arc formation within the Southern Neotethys: Whole-rock, trace element and Sr-Nd-Pb isotopic data from basaltic rocks of the Yüksekova Complex (Malatya-Elazığ, SE Turkey)," *Ofioliti*, vol. 40, no. 1, pp. 57–72, 2015.
[27] S. Özarpacı, B. Kılıç, M. Köküm, and U. Doğan, "GNSS hızlarında kümelemeden topluluk kümelemesine: Meta-kümeleme odaklı bir yaklaşım," *Gümüşhane Üniv. Fen Bil. Derg.*, vol. 13, no. 3, pp. 661–674, 2023.
[28] Y. Yılmaz, F. Şaroğlu, and Y. Güner, "Initiation of the neomagmatism in East Anatolia," *Tectonophysics*, vol. 134, no. 1–3, pp. 177–199, 1987.
[29] A. Koçyiğit, A. Yılmaz, S. Adamia, and S. Kuloshvili, "Neotectonics of East Anatolian Plateau (Turkey) and Lesser Caucasus: Implication for transition from thrusting to strike-slip faulting," *Geodinamica Acta*, vol. 14, no. 1, pp. 177–195, 2001.
[30] J. Jackson and D. McKenzie, "Active tectonics of the Alpine–Himalayan Belt between western Turkey and Pakistan," *Geophys. J. Int.*, vol. 77, no. 1, pp. 185–264, Apr. 1984.
[31] M. Beyarslan and A. F. Bingöl, "Zircon U-Pb age and geochemical constraints on the origin and tectonic implications of Late Cretaceous intra-oceanic arc magmatics in the Southeast Anatolian Orogenic Belt (SE-Turkey)," *J. Afr. Earth Sci.*, vol. 147, pp. 477–497, 2018.
[32] N. Özgül, "Torosların bazı temel jeoloji özellikleri," *Türk. Jeol. Kurumu Bülteni*, vol. 19, no. 1, pp. 65–78, 1976.
[33] H. J. Asutay, "Geology of the Baskil (Elazığ) area and the petrology of Baskil magmatics," *Bull. Miner. Res. Explor.*, vol. 107, no. 107, pp. 51–69, 1986.
[34] C. Koç Taşgin and İ. Türkmen, "Analysis of soft-sediment deformation structures in Neogene fluvio-lacustrine deposits of Çaybağı Formation, Eastern Turkey," *Sediment. Geol.*, vol. 218, no. 1–4, pp. 16–30, 2009.
[35] Ö. Emre, T. Y. Duman, S. Özalp, F. Şaroğlu, Ş. Olgun, H. Elmacı, and T. Çan, "Active fault database of Turkey," *Bull. Earthq. Eng.*, vol. 16, no. 8, pp. 3229–3275.
[36] A. Akbaş, B. Akdeniz, N. Aksay, A. Altun, İ. E. Balcı, V. Bilginer, E. Bilgiç, T. Duru, M. Ercan, T. Gedik, İ. Günay, Y. Güven, İ. H. Hakyemez, H. Y. Konak, N. Papak, İ. Pehlivan, Ş. Sevin, M. Şenel, M. Tarhan, N. Turhan, A. Türkecan, Ü. Ulu, M. F. Uğuz, A. Yurtsever, *et al., 1:1.250.000 Ölçekli Türkiye Jeoloji Haritası*. Ankara, Türkiye: Maden Tetkik ve Arama Genel Müdürlüğü Yayını, 2011.
[37] W. B. Bull and L. D. McFadden, "Tectonic geomorphology north and south of the Garlock fault, California," in *Geomorphology in Arid Regions*. London, U.K.: Routledge, 1977, pp. 115–138.
[38] R. El Hamdouni, C. Irigaray, T. Fernández, J. Chacón, and E. A. Keller, "Assessment of relative active tectonics, southwest border of the Sierra Nevada (southern Spain)," *Geomorphology*, vol. 96, no. 1–2, pp. 150–173, 2008.
[39] R. A. Dar, S. A. Romshoo, R. Chandra, and I. Ahmad, "Tectono-geomorphic study of the Karewa Basin of Kashmir Valley," *J. Asian Earth Sci.*, vol. 92, pp. 143–156, 2014.
[40] Z. Kezer, "Kütahya Grabeni'nin tektonik jeomorfolojisi (Batı Anadolu)," M.S. thesis, Fen Bilimleri Enstitüsü, Hacettepe Üniv., Ankara, Türkiye, 2019.

[41] W. B. Bull, *Tectonic Geomorphology of the Mojave Desert: U.S. Geological Survey Contract Report 14-08-001-G-394*. Menlo Park, CA, USA: Office of Earthquakes, Volcanoes, and Engineering, 1977.
[42] J. V. Pérez-Peña, "GIS-based tools and methods for landscape analysis and active tectonic evaluation," Ph.D. dissertation, Univ. Granada, Granada, Spain, 2009.
[43] J. V. Pérez-Peña, A. Azor, J. M. Azañón, and E. A. Keller, "Active tectonics in the Sierra Nevada (Betic Cordillera, SE Spain): Insights from geomorphic indices and drainage pattern analysis," *Geomorphology*, vol. 119, no. 1–2, pp. 74–87, Jun. 2010.
[44] M. T. Ramírez-Herrera, "Geomorphic assessment of active tectonics in the Acambay graben, Mexican Volcanic Belt," *Earth Surf. Process. Landf.*, vol. 23, no. 4, pp. 317–332, 1998.
[45] A. N. Strahler, "Hypsometric (area-altitude) analysis of erosional topography," *Geol. Soc. Am. Bull.*, vol. 63, no. 11, pp. 1117–1142, 1952.
[46] S. Ciccacci, L. D'Alessandro, P. Fredi, and E. L. Palmieri, "Relations between morphometric characteristics and denudational processes in some drainage basins of Italy," *Z. Geomorphol.*, vol. 36, no. 1, pp. 53–67, 1992.
[47] A. Sağlam Selçuk, "Evaluation of the relative tectonic activity in the eastern Lake Van basin, East Turkey," *Geomorphology*, vol. 270, pp. 9–21, Oct. 2016.
[48] F. Giaconia, G. Booth-Rea, J. M. Martínez-Martínez, J. M. Azañón, J. V. Pérez-Peña, J. Pérez-Romero, and I. Villegas, "Geomorphic evidence of active tectonics in the Sierra Alhamilla (eastern Betics, SE Spain)," *Geomorphology*, vol. 145–146, pp. 90–106, 2012.
[49] A. Karataş, "Karasu Çayı havzasının hidrografik planlaması," Ph.D. dissertation, Sosyal Bilimler Enstitüsü, İstanbul Üniv., İstanbul, Türkiye, 2014.
[50] S. Salman, "Yeşilyurt Fayı'nın göreceli tektonik evriminin morfometrik indislerle belirlenmesi," M.S. thesis, Lisansüstü Eğitim Enstitüsü, Bitlis Eren Üniv., Bitlis, Türkiye, 2024.
[51] M. Uzun, "Lale Dere (Yalova) Havzası'nın jeomorfolojik özelliklerinin jeomorfometrik analizlerle incelenmesi," *Route Educ. Soc. Sci. J.*, vol. 1, no. 3, pp. 72–88, 2014.
[52] F. Ü. Çelik, "Erkilet Fay Zonu'nun paleosismolojik ve morfotektonik özellikleri (Kayseri, Orta Anadolu-Türkiye)," M.S. thesis, İstanbul Teknik Üniv., İstanbul, Türkiye, 2023.
[53] M. P. Awasthi, "Application of ArcHydro tool, geospatial technologies and digital elevation model for watershed modeling: A case of Nepal Himalaya," *Int. J. Environ. Geoinformatics*, vol. 12, no. 1, pp. 1–14, 2025.
[54] S. A. Mahmood and R. Gloaguen, "Appraisal of active tectonics in Hindu Kush: Insights from DEM derived geomorphic indices and drainage analysis," *Geosci. Front.*, vol. 3, no. 4, pp. 407–428, 2012.
[55] J. T. Hack, "Stream-profile analysis and stream-gradient index," *J. Res. U.S. Geol. Surv.*, vol. 1, no. 4, pp. 421–429, 1973.
[56] D. Piacentini, F. Troiani, T. Servizi, O. Nesci, and F. Veneri, "SLIX: A GIS toolbox to support along-stream knickzones detection through the computation and mapping of the stream length-gradient (SL) index," *ISPRS Int. J. Geo-Inf.*, vol. 9, no. 2, p. 69, 2020.
[57] E. A. Keller and N. Pinter, *Active Tectonics: Earthquakes, Uplift, and Landscapes*, 2nd ed. Upper Saddle River, NJ, USA: Prentice Hall, 2002.
[58] D. L. Wells and K. J. Coppersmith, "New empirical relationships among magnitude, rupture length, rupture width, rupture area, and surface displacement," *Bull. Seismol. Soc. Am.*, vol. 84, no. 4, pp. 974–1002, 1994.
[59] T. K. Rockwell, E. A. Keller, M. N. Clark, and D. L. Johnson, "Chronology and rates of faulting of Ventura River terraces, California," *Geol. Soc. Am. Bull.*, vol. 95, no. 12, pp. 1466–1474, 1984.
[60] A. Khalifa, Z. Çakir, L. Owen, and Ş. Kaya, "Morphotectonic analysis of the East Anatolian Fault, Turkey," *Turkish J. Earth Sci.*, vol. 27, no. 2, 2018.
[61] S. Mutlu, "Iğdır Fay Zonu'nun Doğu Anadolu kısalmalı tektonik bloğu içerisindeki önemi ve morfotektonik özellikleri," *Türkiye Jeol. Bülteni*, vol. 68, no. 2, pp. 1–41, 2025.